# ESTIMATION OF MANGROVE FRACTIONAL COVER FROM MULTISPECTRAL AND HYPERSPECTRAL DATA USING MIXTURE TUNED MATCHED FILTERING

A. C. Blanco* [1,2], C.R. Perez [1,2]
[1] Philippine Space Agency, Diliman, Quezon City 1101, Philippines – ariel.blanco@philsa.gov.ph
[2] Department of Geodetic Engineering, College of Engineering, University of the Philippines Diliman, Quezon City 1101, Philippines – acblanco@up.edu.ph

**KEY WORDS:** Mangroves, Landsat, PRISMA, MNF, MTMF, Regression, MVI, EMVI

**ABSTRACT:**

Mangroves provide various ecosystem services and contribute to climate change adaptation being one of the blue carbon ecosystems. The extents of mangroves are mapped and monitored using commonly available multispectral images, such as Landsat and Sentinel-2, to detect and assess gains and losses. However, this presence or absence per pixel based on crisp classification or index thresholding offers limited information on the dynamics of mangrove growth or decline. In this paper, we evaluated the use of Mixture Tuned Matched Filtering (MTMF) in estimating mangrove fractional cover (MFC) from multispectral (Landsat-8) and hyperspectral (PRISMA) satellite images. We also examined the utility of the mangrove vegetation index (MVI) and enhanced MVI (EMVI) for this purpose. The images were first denoised using Minimum Noise Fraction (MNF). MTMF was then separately applied to the sets of MNF bands, excluding noise bands, to generate Matched Filtering (MF) Score and Infeasibility layers. The endmember (mangrove) spectrum was extracted from a pixel identified using pixel purity index (PPI) and examination of high-resolution Google Earth base image, from which detailed mangrove extents were also delineated. A 30-m vector grid file was created and populated with MFC, MF Score, and Infeasibility values using zonal analysis. Correlation analysis, exploratory regression, and ordinary least squares (OLS) regression were performed. MF Score is moderately and positively correlated with MFC. In contrast, Infeasibility, MVI, and EMVI are uncorrelated or very weakly correlated with MFC. MFC can be estimated using an OLS model with MF Score and Infeasibility as explanatory variables. The performance of the PRISMA-based model ($R^2_{Adj}$=0.30, AIC=98643.20) was found to be better than the Landsat-8-based model ($R^2_{Adj}$=0.36, AIC=97428.89).

## 1. INTRODUCTION

The availability of hyperspectral images is increasing, whether free or commercial. This can be partly attributed to the efforts of NASA, DLR, ASI, and other space agencies. With these hyperspectral satellite images, various applications are assessed vis-à-vis multispectral satellite images, examining whether the use of hyperspectral images provide significant accuracy improvements at various levels of information. As an example, Kokal et al. (2022) used PRISMA and LANDSAT-9 in land cover classification using Support Vector Machine classifier and PRISMA was found to produce slightly better overall accuracy. Land cover classes included industrial area, roads, residential area, airport, sea, forest, vegetation, and barren land. Kokal et al. (2022) concluded that this was due to the higher spectral resolution of PRISMA compared to LANDSAT-9's spectral resolution of 20–180 nm. In forest type discrimination, PRISMA yielded better results compared to Sentinel-2 Multi-Spectral Instrument (MSI) using two different nomenclature systems and four separability metrics (Vangi et al., 2021). The performance increased alongside the increasing complexity of the nomenclature system. PRISMA, relative to Sentinel-2, yielded an average improvement of 40% in discriminating between two forest categories (coniferous vs. broadleaves) and 102% for the case of five forest types based on main tree species groups. This highlights the utility of hyperspectral images in a continuum from 400 and 2500 nm, with high spectral resolution ($\leq$12 nm), in detailed mapping of vegetation, including mangroves.

Mangroves provide various ecosystem services including serving as habitats to many species, the protection of shorelines, and the sequestration and storage of huge amounts of carbon the biomass and sediments of mangrove forests. Despite these ecosystem services and the increasing attention, mangroves are continually threatened by anthropogenic activities, typhoons, and climate change impacts. This underscores the critical importance of mapping and monitoring mangroves. Lassalle et al. (2023) emphasized that "remote sensing will undoubtedly become an essential tool to monitor the diversity of these endangered ecosystems in the future" and "efforts should concentrate on evaluating the capabilities of new and upcoming instruments and multisource data combination to improve mangrove species mapping and, more broadly, to meet conservation goals".

Remote sensing has been used in mapping extents, percentage of canopy closure, health, and species distribution in mangrove forests (Kuenzer et al., 2011). Hati et al. (2021) evaluated the performance of multispectral (Landsat 8 OLI and Sentinel-2) and hyperspectral (AVIRIS-NG and Hyperion) images in discriminating mangrove species. The hyperspectral classification yielded higher accuracies (AVIRIS-NG, 87.61%; Hyperion, 81.98%) compared to those utilizing Landsat 8 OLI (76.42%) and Sentinel-2 (79.81%). Beyond genus-level, AVIRIS-NG hyperspectral (20-m resolution) can be used to satisfactorily classify mangrove species in a complex mangrove forest. Recent advances use a multitask convolutional neural network to achieve accurate classification (up to 97%) using the most comprehensive dataset of optical imagery (including hyperspectral) over a mangrove forest (Lasalle et al., 2023). Based on Lasalle et al.

* Corresponding author

(2023), "multispectral imagery performs well at very-high to high resolutions (up to 10–20 m) but suffers from the lack of spectral information at medium resolution (30 m)". Utilizing hyperspectral imagery, the best results were obtained at sub-metric resolution (0.5 m) while satisfactory results (≥ 85% accuracy) were achieved at 30-m resolution.

While mapping and monitoring extents is important, mangrove extent information does not include variations of mangrove cover within these "boundaries". Furthermore, with the mixed pixel problem common in moderate and low-resolution images, low fractional cover mangrove areas are commonly excluded in mangrove extent mapping. This is a severe limitation when monitoring growth, expansion, and even decline in mangrove cover. Canopy closure/cover or fractional cover data provide information on the dynamics and health status of mangrove stands and are useful for assessing impacts of drivers and pressures on mangroves (Kuenzer et al., 2011, Morsef and Smith, 2017). To date, only a few studies on estimating fractional or percent mangrove cover have been carried out. Morsef and Smith (2017) utilized linear spectral unmixing on a stack of seven indices derived from Landsat-8 imagery to estimate mangrove canopy cover. The difficulty associated with spectral unmixing is the provision of most, if not all, endmember spectra. In the approach of Morsef and Smith (2017), the identification and extraction of endmember spectra from the image becomes even more difficult as the spectra considered is composed of the values of the seven indices and not the reflectance.

This paper evaluated the use of Mixture Tuned Matched Filtering (MTMF) in estimating mangrove fractional cover (MFC). This method was chosen as MTMF only requires at least one endmember spectra. MTMF has been used in estimating abundance of mangrove species using EO-1 Hyperion data (Demuro and Chisholm, 2003). The interactive approach using scattergram was utilized to identify locations of selected mangrove species. However, Demuro and Chisholm (2003) did not estimate the percentage of mangrove cover. In this paper, we employed linear regression analysis to generate MFC models utilizing MTMF layers generated from Landsat-8 and from PRIMA hyperspectral images. Such models can be used to assess in more detail how mangrove forest grow and diminish or recover from damages.

This paper also examined whether the mangrove vegetation index (Baloloy et al., 2020) for multispectral data and the enhanced mangrove vegetation index (Yang et al. 2022) for hyperspectral data can be used for mangrove fractional cover estimation.

## 2. DATA AND METHODOLOGY

### 2.1 Data Used in this Study

This study utilized Landsat-8 and PRISMA (PRecursore IperSpettrale della Missione Applicativa or Hyperspectral Precursor of the Application Mission) images covering portion of Bani, Pangasinan in the Philippines (Figure 1). The area was chosen since it has various densities of mangrove cover ranging from no mangroves to full cover of mangroves.

PRISMA, a satellite of the Italian Space Agency, generates hyperspectral images comprising of 173 bands within in the short-wave infrared (SWIR) portion, specifically 920–2500 nm, and 66 bands within the visible near-infrared (VNIR) portion, specifically 400–1010 nm, of the light spectrum (Vangi et al., 2021). The spatial resolution is 30 m the spectral resolution is $\leq$12 nm. It also produces 5-m panchromatic images covering the wavelength range of 400–700 nm. Shaik, Periasamy, and Zeng (2023) noted that PRISMA hyperspectral images have been utilized in various applications including forest fuel mapping, forest discrimination, burned area mapping, prediction of methane emissions, agricultural applications, mapping of soil moisture, soil organic matter, and soil organic carbon, water quality, and geological applications. However, compared to other applications, PRISMA images have greater potential to extract vegetation biophysical parameters, owing to its higher reflectance spectra and comprehensive spectral coverage (Shaik, Periasamy, and Zeng, 2023).

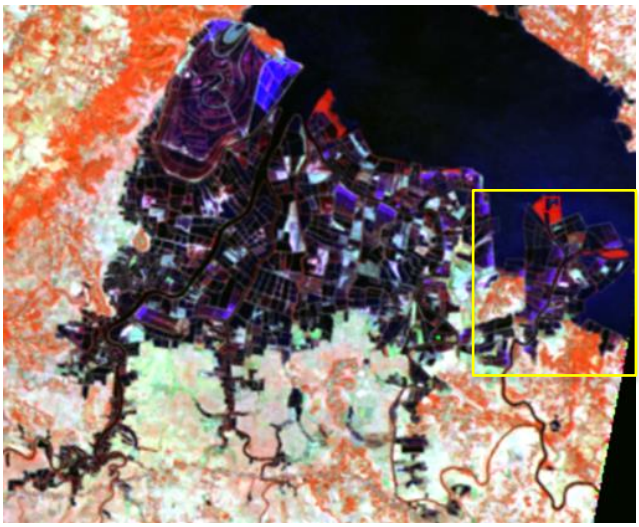

**Figure 1.** False color composite from PRISMA hyperspectral bands covering the study site (mangroves and fishpond areas bounded by the yellow box) in the Municipality of Bani, Province of Pangasinan, Philippines. The study site has different sizes of mangrove clusters shown as dark red areas near water bodies and fishponds.

Various levels of PRISMA products are available: Level 0, Level 1, and Level 2. Level 0 is raw data in binary files, including instrument and satellite ancillary data. Level 1 images are hypercubes and panchromatic radiance images radiometrically (top-of-atmosphere) and geometrically calibrated. Level 2 has four sub-levels: L2A, L2B (geolocated on-ground radiance), L2C (geolocated reflectance), and L2D (geocoded on-ground reflectance) (Vangi et al., 2021, Cogliati et al., 2021). This study utilized PRISMA L2D image acquired on 4 March 2020 and provided by ASI.

The Landsat-8 image (surface reflectance) was acquired on 18 March 2020. For the delineation of the "true" extents of mangroves for fractional cover estimation, mangroves were delineated from high-resolution satellite images available in Google Earth.

### 2.2 Methodology

The methodological flow diagram is shown in Figure 2. The estimation of the fractional cover of mangroves in this study is based on the hypothesis that the Matched Filtering (MF) score can be used to measure the abundance of "pure" mangroves and hence, it can be used for the estimating MFC.

***Denoising***

The PRISMA and Landsat-8 images were each subjected to Minimum Noise Fraction (MNF) transformation in ENVI. MNF is a well-known technique for denoising hyperspectral imagery. A noisy data cube is transformed into MNF output images with

steadily increasing noise levels or steadily decreasing image quality (Luo et al., 2016). Through MNF, the components and their varying contrinution to the spectral variance of the original data and the noise present in the data are generated (Keshava & Mustard, 2002). In terms of noise, many bands (>20) of PRISMA contain too much noise (>50%) (Shaik et al., 2022) and irregular noise values can be found in selected bands (Shaik et al., 2021). Noise bands in the MNF were identified and excluded in subsequent processing stages.

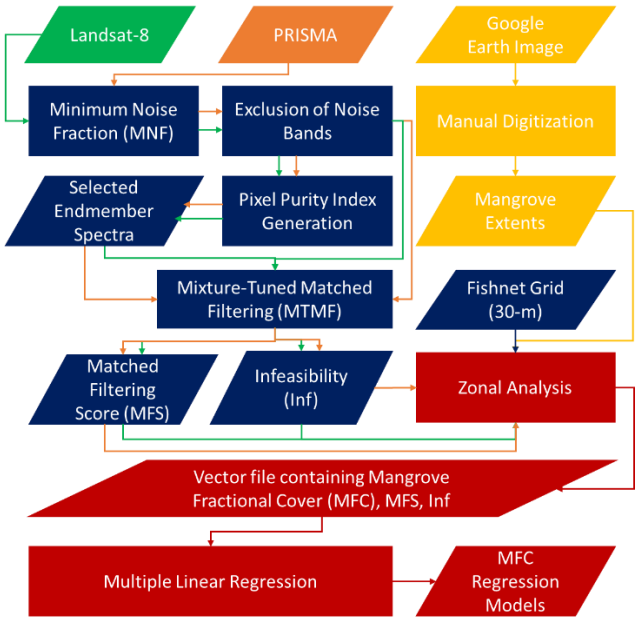


**Figure 2.** Methodological flow diagram for estimating mangrove fractional cover from Landsat-8 and PRISMA images.

***Endmenber Extraction***

The process of finding the materials in the pixel under consideration is called endmember extraction. One of the two common assumptions in endmenber extraction is the assumption that there are a few pixels which are pure (i.e., composed of only one material). For this study, Pixel Purity Index (PPI), one of the algorithms based on the assumption of pure pixel (Keshava, 2003), was utilized to identify the purest mangrove pixel which can be used as source of the spectra in MNF space. The PPI step, however, is optional as it is easy to identify pixels with full mangrove cover based on high-resolution satellite or aerial images. This endmember spectra is then used in Mixture-Tuned Matched Filtering.

***Mixture-Tuned Matched Filtering (MTMF)***

MTMF partially unmixes pixel spectra according to a user-defined endmember. The reference endmember spectrum is matched to the pixel spectra by maximizing the endmember response and masking the background unknown response (ENVI, 2001). The process produces two output layers, namely, the Matched Filtering (MF) Score and the Infeasibility. The results indicate the degree to which the endmember was matched to the pixel spectra and the approximate sub-pixel response of the endmember. The Infeasibility layer can be used to identify the 'false positives' as high infeasibility values mean erroneous matching to the endmember. We suppose that Infeasibility can be used to make the estimation of fractional cover from MF Score more accurate.

MTMF was applied to the non-noisy MNF bands derived from the Landsat-8 and PRISMA images using the pure mangrove spectra as identified using PPI and reference to high-resolution satellite image. The MF Score and Infeasibility (see Figure 3 for PRISMA) can jointly be used to identify mangrove pixels and delineate the extents of mangroves. This is typically done by examining the scatter plot of these two variables. Scatter points of high MF Score and low Infeasibility values are mangroves. However, accurately identifying the decision boundary in the scatter plot to delineate varying amounts of the endmember, mangroves in this case, is difficult. In this study, the mangrove vegetation index (MVI) and the enhanced mangrove vegetation index (EMVI) were used to delineate mangrove using the Landsat-8 and PRISMA data, respectively.

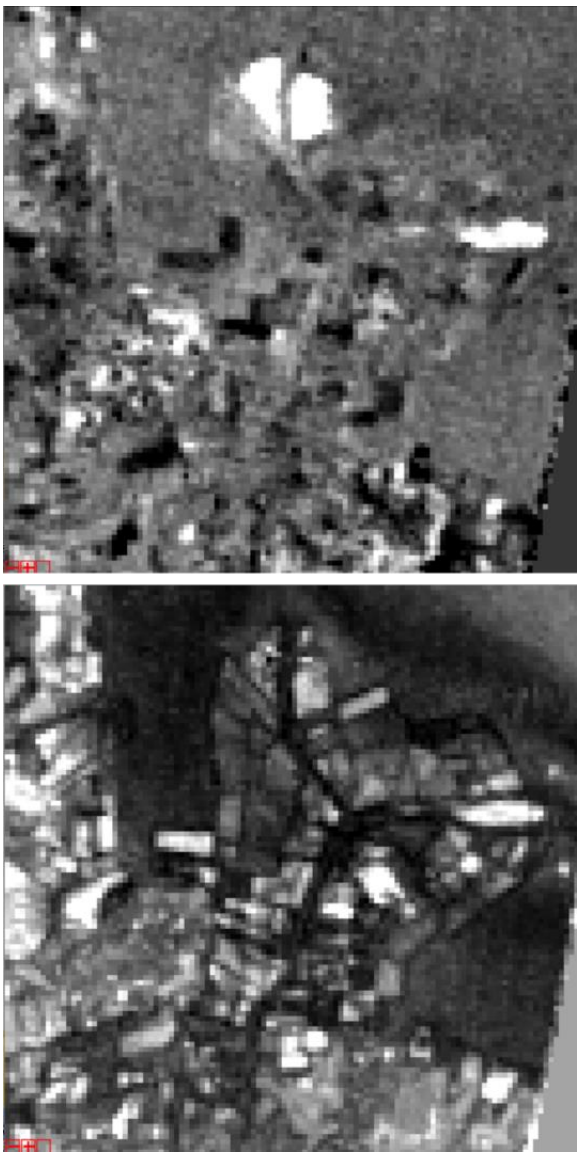

**Figure 3.** Matched Filtering (MF) score (top) and Infeasibility (bottom) layers generated from the PRISMA hyperspectral image. Mangroves are generally those with high MF score and low Infeasibility values.

***Mangrove Extents from High-resolution Image***

Image interpretation of a Google Earth base map was conducted to generate accurate delineations of mangroves in the study area. Moreover, the use of Google Street View was also used in

conjunction to Google Earth base map to ensure that the manually delineated areas are mangrove stands. The MVI and EMVI layers were also used as reference. These mangrove extents data, as shown in Figure 4, were used to calculate the "true" mangrove fractional cover (MFC_true) within 30-m grid cells using Zonal Analysis. Note that these delineations are not exhaustive, i.e., some small and narrow cluster may have been missed.

**Figure 4.** Mangrove extents (yellow) delineated from Google Earth base image as shown.

***Zonal Analysis***

A fishnet grid with cell of 30 m and aligned with the Landsat-8 and PRISMA images was created in ArcGIS Pro. Each cell was then populated with values from the following value rasters, namely, MF Score and Infeasibility images, and the raster equivalent of the detailed mangrove extents delineated previously.

***Statistics Analysis and Modelling***

Pearson correlation analysis was performed to assess the linear relationship between MFC and other variables, including the MVI and EMVI. Exploratory Regression (ER) and Ordinary Least Square (OLS) Regression (OLSR) with MFC_true as the dependent variable were implemented in ArcGIS Pro. ER evaluates all possible combinations of explanatory or independent variables in models that best explains the variability in the dependent variable. OLSR generates OLS models using the selected independent variables and outputs variables statistical reports and layers to evaluate model performance. The independent variables considered are the following: MF Score, Infeasibility, and MVI or EMVI as applicable.

## 3. RESULTS AND DISCUSSION

### 3.1 Correlation with MFC

MVI and EMVI are not correlated with MFC with R equal to -0.049 and 0.005, respectively. If only non-zero MFC values are considered, the MFC remains uncorrelated with MVI (R= -0.035) and EMVI (R= -0.022). In Baloloy et al. (2020), MVI was found to be correlated with Leaf Area Index (LAI) and Fractional Vegetation Cover (FVC) generated from Sentinel-2 using biophysical models implemented in SNAP. FVC corresponds to the gap fraction for nadir direction and can provide quantitative information of the vegetation coverage status on the ground (Li et al., 2015). It should be noted that Baloloy et al. (2020) implemented the correlation analysis using MVI-identified mangrove pixels obtained from two forest types: riverine and fringe mangrove forests. These mangrove pixels perhaps have greater than 40% mangrove cover. However, successively increasing the lower MFC limit did not result to significantly increase in correlation.

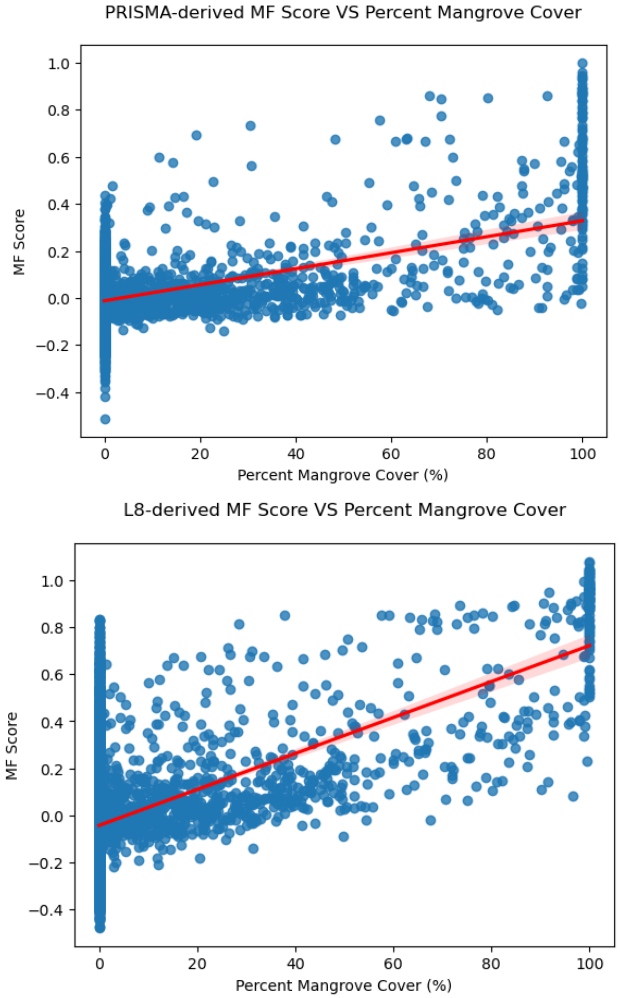


**Figure 5.** Scatter plot of percent mangrove cover or MFC with PRISM-derived MF Score (top) and Landsat-8-derived MF Score (bottom).

On the other hand, MF Score has moderate positive correlation with MFC. The Pearson's coefficient of correlation between PRISMA-derived MF Scores and <FC is R = 0.59 (p-value= 0.0). This is slightly higher than the correlation for the case of Landsat-8-derived MF Scores at R = 0.53 (p-value= 0.0). Both Infeasibility are weakly correlated with MFC.

### 3.2 Spatial Variation of MF Score and Infeasibility

The general distribution of mangroves, especially those dense mangrove stands, was captured by both MF Score layers (Figure 6). The potentially mangrove areas in PRISMA MF Score seems to be more reasonably correct compared to the spatial distribution depicted in Landsat MF Score. It appears that more "less likely" mangrove areas are shown in the Landsat-8 MF Score layer. These areas are of low MF Score based on PRISMA. However, the line of mangroves bounding the fishponds are more evident in Landsat-

8 MF Score layer. The PRISMA Infeasibility compensates for this as these lines of mangroves are shown in very low values. Overall, PRISMA Infeasibility is higher in many parts of the study area, particularly in areas with mangrove or with other types of vegetation.

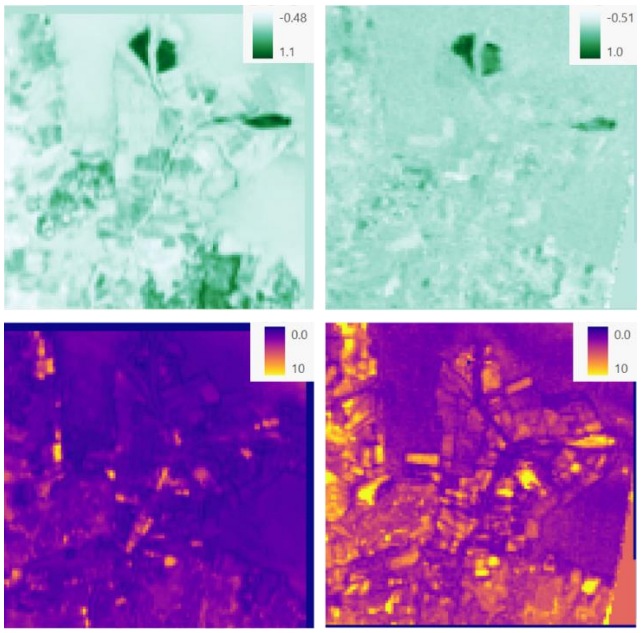


**Figure 6.** MF Score (top) and Infeasibility (bottom) layers derived from Landsat-8 image (left) and PRISMA hyperspectral image (right).

### 3.3 Regression Models

The inclusion of MVI and EMVI into the linear regression models was rejected with the P-value being much greater than the confidence level of 0.95. MVI and EMVI did not add explanatory power to the OLS models. Their inclusion resulted in models with significantly higher Akaike Information Criteria (AIC). Thus, Table 1 shows only the models with MS Score only and those with the corresponding Infeasibility included. The best model is based on PRISMA MF Score and Infeasibility with the highest Adjusted $R^2$ and lowest AIC. The removal of PRISMA Infeasibility did not change the Adjusted $R^2$ but it increased the AIC slightly.

| Model | Adjusted R-Squared | Akaike Information Criteria (AIC) |
|---|---|---|
| L8_MF Score | 0.28 | 98985.97 |
| L8_MF Score, Infeasibility | 0.30 | 98643.20 |
| PRISMA_MF Score | 0.36 | 97483.20 |
| PRISMA_MF Score, Infeasibility | **0.36** | **97428.89** |

**Table 1.** Linear regression models for estimating mangrove fractional cover using mixture tuned matched filtering on Landsat-8 (L8) and PRISMA data. The models utilized either or both Matched Filtering Score (MF Score) and Infeasibility.

The PRISMA MTMF-based OLS model was able to capture the spatial variation of MFC better compared to the OLS model based on Landsat MTMF. The dense mangrove areas were mapped, though areas with 100% cover were underestimated to around 85%. In the Landsat-8-based estimation, these areas were severely underestimated to just around 45%. This underestimation can be addressed by using other pixels with 100% cover and with the lower or lowest PPI value.

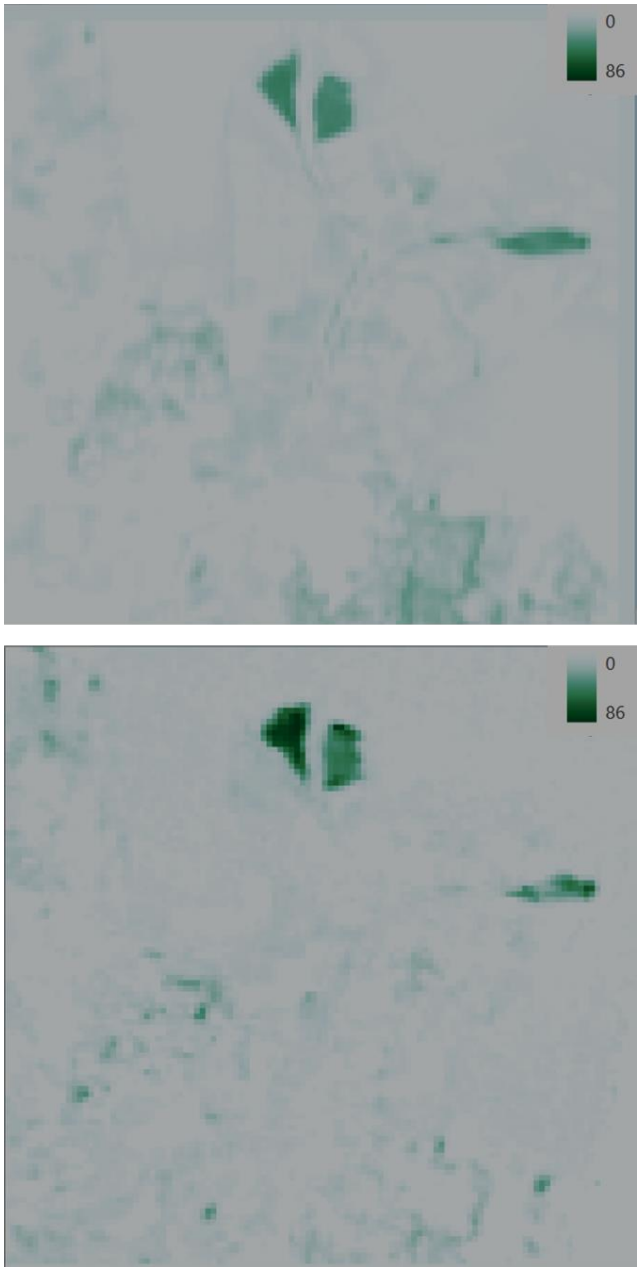


**Figure 7.** Mangrove percentage or fractional cover estimated using OLS regression models with MF Score and Infeasibility as explanatory variables based on Landsat-8 image (top) and PRISMA hyperspectral image (bottom).

As noted earlier, the lines of mangroves along the boundaries of fishponds and on riverbanks were better captured in MF Score as well as in the predicted MFC based on the Landsat-8 image. These lines are not evident in the MFC predicted from PRISMA. This is possibly due to the noise or spatial artifacts which have remained even after the denoising through MNF.

The predicted MFC layers were able to show mangrove areas which were excluded in the manual digitization from Google Earth base image. These areas need further validation through field surveys.

## 4. SUMMARY, CONCLUSIONS AND RECOMMENDATIONS FOR FUTURE WORK

This study addressed an important topic related to mangrove mapping and monitoring, highlighting the significance of assessing fractional cover for understanding the dynamics and health of mangrove stands. The use of remote sensing data, specifically Landsat-8 and PRISMA, for estimating mangrove fractional cover is a relevant and practical approach. The paper introduced the Mixture Tuned Matched Filtering (MTMF) method and applied linear regression analysis to generate fractional mangrove cover models. This combination of methods has the potential to provide valuable insights into the abundance and distribution of mangroves.

Regression models based on the MTMF of PRISMA hyperspectral image provided better results compared to those based on Landsat-8 MTMF. Severe underestimations were observed in the Landsat-8-based predicted MFC. However, narrow mangrove areas were captured better in Landsat-based models.

Recommendations for future work include (1) improved noise removal, perhaps through filtering in the frequency domain in addition to the MNF, (2) experiments on the extraction of endmember spectra, and (3) explore other layers which can assist in explaining the variability in mangrove fractional or percentage cover.

## REFERENCES

Baloloy, A.B., Blanco, A.C., Sta. Ana, R.R.C., Nadaoka, K. 2020. Development and application of a new mangrove vegetation index (MVI) for rapid and accurate mangrove mapping. ISPRS Journal of Photogrammetry and Remote Sensing. 166, 95-117. https://doi.org/10.1016/j.isprsjprs.2020.06.001

Cogliati, S.; Sarti, F.; Chiarantini, L.; Cosi, M.; Lorusso, R.; Lopinto, E.; Miglietta, F.; Genesio, L.; Guanter, L.; Damm, A.; et al. The PRISMA Imaging Spectroscopy Mission: Overview and First Performance Analysis. Remote. Sens. Environ. 2021, 262.

Demuro, M.; Chisholm, L. Assessment of Hyperion for Characterizing Mangrove Communities. In Proceedings of the International Conference the AVIRIS 2003 Workshop, Pasadena, CA, USA, 24 February 2003; pp. 18–23.

ENVI. 2001. ENVI (Environment for Visualizing Images) User's Guide: Images to Information. Research Systems, Inc., Boulder CO.

Jyoti Prakash Hati, Sourav Samanta, Nilima Rani Chaube, Arundhati Misra, Sandip Giri, Niloy Pramanick, Kaushik Gupta, Sayani Datta Majumdar, Abhra Chanda, Anirban Mukhopadhyay, Sugata Hazra, Mangrove classification using airborne hyperspectral AVIRIS-NG and comparing with other spaceborne hyperspectral and multispectral data, The Egyptian Journal of Remote Sensing and Space Science, Volume 24, Issue 2, 2021, pages 273-281, ISSN 1110-9823, https://doi.org/10.1016/j.ejrs.2020.10.002.

Keshava, N. & Mustard J.F. 2002. Spectral unmixing. IEEE Signal Processing Magazine 19, 44–57.

Keshava, N.: A survey of spectral unmixing algorithms. Lincoln Lab. J. 14, 55–78 (2003)

Li, Y., Wang, H., Li, X.B. 2015. Fractional vegetation cover estimation based on an improved selective endmember spectral mixture model. PLoS ONE 10. 4. https://doi.org/10.1371/journal.pone.0124608

Luo, G., Chen, G., Tian, L., Qin, K., & Qian, S.E. 2016. Minimum Noise Fraction versus Principal Component Analysis as a Preprocessing Step for Hyperspectral Imagery Denoising, Canadian Journal of Remote Sensing, 42:2, 106-116, DOI: 10.1080/07038992.2016.1160772

Tuzcu Kokal, A., İsmailoğlu, İ., and Musaoğlu, N.: COMPARISON OF LANDSAT-9 AND PRISMA SATELLITE DATA FOR LAND USE / LAND COVER CLASSIFICATION, Int. Arch. Photogramm. Remote Sens. Spatial Inf. Sci., XLVI-M-2-2022, 197–201, https://doi.org/10.5194/isprs-archives-XLVI-M-2-2022-197-2022, 2022.

Kuenzer, Claudia, Andrea Bluemel, Steffen Gebhardt, Tuan Vo Quoc, and Stefan Dech. 2011. "Remote Sensing of Mangrove Ecosystems: A Review" Remote Sensing 3, no. 5: 878-928. https://doi.org/10.3390/rs3050878

Monsef, H. A., Smith, S. E., 2017. A new approach for estimating mangrove canopy cover using Landsat 8 imagery. Computers and Electronics in Agriculture 135 (2017) 183–194. http://dx.doi.org/10.1016/j.compag.2017.02.007.

Shaik, R.U.; Giovanni, L.; Fusilli, L. New Approach of Sample Generation and Classification for Wildfire Fuel Mapping on Hyperspectral (Prisma) Image. In Proceedings of the International Geoscience and Remote Sensing Symposium (IGARSS), Brussels, Belgium, 11–16 July 2021; Institute of Electrical and Electronics Engineers Inc.: New York, NY, USA, 2021; pp. 5417–5420.

Shaik, R.U.; Laneve, G.; Fusilli, L. An Automatic Procedure for Forest Fire Fuel Mapping Using Hyperspectral (PRISMA) Imagery: A Semi-Supervised Classification Approach. Remote Sens. 2022, 14, 1264.

Shaik, R.U., Periasamy, S., Zeng,W., 2023. Potential Assessment of PRISMA Hyperspectral Imagery for Remote Sensing Applications. Remote Sens. 2023, 15, 1378. https://doi.org/10.3390/rs15051378

Vangi, E., D'amico, G., Francini, S., Giannetti, F., Lasserre, B., Marchetti, M., Chirici, G., 2021. The New Hyperspectral Satellite Prisma: Imagery for Forest Types Discrimination. Sensors 2021, 21, 1–19.

Yang, G., 2022. Enhanced mangrove vegetation index based on hyperspectral images for mapping mangrove. ISPRS Journal of Photogrammetry and Remote Sensing189: 236-254